Available online at www.sciencedirect.com
ScienceDirect
Biochimica et Biophysica Acta 1768 (2007) 1681–1690
Biochimica et Biophysica Acta BBA
www.elsevier.com/locate/bbamem

The ergosterol biosynthesis inhibitor zaragozic acid promotes vacuolar degradation of the tryptophan permease Tat2p in yeast

Katsue Daicho [1], Hironori Maruyama [1], Asuka Suzuki, Masaru Ueno [2], Masahiro Uritani, Takashi Ushimaru *

Faculty of Science, Shizuoka University, Shizuoka 422-8529, Japan

Received 28 September 2005; received in revised form 13 March 2007; accepted 15 March 2007
Available online 31 March 2007

Abstract

Ergosterol is the yeast functional equivalent of cholesterol in mammalian cells. Deletion of the *ERG6* gene, which encodes an enzyme catalyzing a late step of ergosterol biosynthesis, impedes targeting of the tryptophan permease Tat2p to the plasma membrane, but does not promote vacuolar degradation. It is unknown whether similar features appear when other steps of ergosterol biogenesis are inhibited. We show herein that the ergosterol biosynthesis inhibitor zaragozic acid (ZA) evoked massive vacuolar degradation of Tat2p, accompanied by a decrease in tryptophan uptake. ZA inhibits squalene synthetase (SQS, EC 2.5.1.21), which catalyzes the first committed step in the formation of cholesterol/ergosterol. The degradation of Tat2p was dependent on the Rsp5p-mediated ubiquitination of Tat2p and was not suppressed by deletions of *VPS1*, *VPS27*, *VPS45* or *PEP12*. We will discuss ZA-mediated Tat2p degradation in the context of lipid rafts.

Keywords: Ergosterol; Zaragozic acid; Rapamycin; Tryptophan; Tat2p

1. Introduction

In the budding yeast *Saccharomyces cerevisiae*, the tryptophan permease Tat2p is synthesized in the endoplasmic reticulum (ER) and trafficked via the secretory pathway to the plasma membrane [1–3]. However, proteolytic degradation of Tat2p in the vacuole is evoked in response to various environmental conditions, including nutrient starvation, high tryptophan, and high pressure stress [1–5]. Especially, Tat2p degradation and a resultant decrease in tryptophan uptake activity become the Achilles' heel of yeast growth under high-pressure stress conditions [4]. This vacuolar targeting is dependent on the ubiquitination of Tat2p.

Ergosterol is the yeast functional equivalent of cholesterol in mammalian cells. Ergosterol biosynthesis requires a large number of enzymes encoded by *ERG* genes in yeast (see Fig. 1). Yeast mutants with deletion of *ERG6*, which encodes an enzyme required for a late step of ergosterol biogenesis, are defective in tryptophan uptake [6]. The *ERG6*-deleted strain cells are viable in a tryptophan autotrophic (*TRP1*), but not auxotrophic (*trp1*), background and the lethality of the *erg6 trp1* cells is suppressed by addition of high concentrations of tryptophan [2]. These facts indicate that tryptophan uptake is critical for viability of the *erg6* mutant. Interestingly, vacuolar degradation of Tat2p was not, however, promoted in this mutant in the presence of sufficient tryptophan, although targeting of Tat2p to the plasma membrane was compromised [2]. In this mutant, vacuolar degradation of Tat2p was clearly observed only when the concentration of tryptophan in the medium was low [2]. It is unknown whether similar features would appear if other steps of ergosterol biogenesis were inhibited.

Squalene synthetase (SQS, EC 2.5.1.21), encoded by *ERG9* in yeast, catalyzes the conversion of farnesyl pyrophosphate to squalene (Fig. 1). This reaction represents the first committed step in the formation of cholesterol and related sterols and is thought to represent a major control point of isoprene and sterol

* Corresponding author. Fax: +81 54 238 0986.
E-mail address: sbtushi@ipc.shizuoka.ac.jp (T. Ushimaru).
[1] K. Daicho and H. Maruyama contributed equally to this paper.
[2] Present address: Department of Molecular Biotechnology, Graduate School of Advanced Sciences of Matter, Hiroshima University, 1-3-1 Kagamiyama, Higashi-Hiroshima 739-8530, Japan.

0005-2736/$ - see front matter © 2007 Published by Elsevier B.V.
doi:10.1016/j.bbamem.2007.03.022

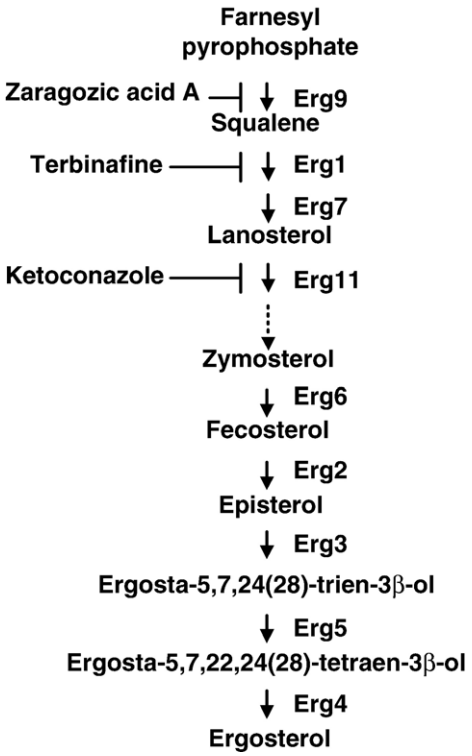

Fig. 1. Sterol synthesis pathway and inhibitors in yeast.

biosynthesis in eukaryotes [7–11]. The fungal metabolite zaragozic acid (ZA) acts as a competitive inhibitor of SQS. It is likely that *erg6*-deleted mutants can grow by producing zymosterol (see Fig. 1), whereas *erg9* mutations (or inhibition) are lethal, probably because of the lack of such sterols. Here we show that ZA promoted vacuolar degradation of Tat2p, unlike *erg6* mutation. ZA-stimulated vacuolar targeting of Tat2p was mediated by ubiquitination.

2. Materials and methods

2.1. Strains, plasmids, and media

For experiments with sterol inhibitors, wild-type strain KMY1005 (SCU7; *MATα leu2-3,112 ura3-52 his3Δ200 trp1Δ901 lys2-801*) [12] and its derivatives SCU645 (*pep4::loxP-kanMX4-loxP*), SCU757 (*vps45::hphMX4*), SCU718 (*vps1:: loxP-kanMX4-loxP*), SCU874 (*vps27:: loxP-kanMX4-loxP*), SCU620 (*end4::loxP-kanMX4-loxP*), SCU755 (*pep12::hphMX*) and SCU649 (*rsp5:: loxP-kanMX4-loxP* [YCp-rsp5-1]) were used. Deletions of *PEP4*, *VPS45, VPS1, VPS27, PEP12*, *RSP5* and *END4* were done by the one-step PCR-mediated gene disruption method [13–15]. To examine the effect of deletion of *ERG6*, we used the wild-type (RH2886; *MATα trp1 ade2 ura3 leu2 bar1*) and *erg6 trp1* (SCU816), which was obtained by mating of *erg6Δ* (*erg6::LEU2*; RH3622) [16] with the *trp1* strain (RH2886). Plasmids pRS414 (*TRP1 CEN*) [17], pHA2-TAT2 (*URA3* 2 μ), pHA2-TAT2(5KR) (*URA3* 2 μ) [1, 18] and YCplac33-rsp5-1 (*URA3 CEN*) [3] were used. The compositions of adenine-containing rich medium (YPAD) and synthetic minimal medium (SD) were described previously [18]. Normal SD medium contained 20 μg/ml of tryptophan.

2.2. Western blot analysis

Cells (a 25-ml culture in SD grown to mid-log phase) expressing HA2-TAT2 or HA2-TAT2(5KR) were disrupted in 200 μl of lysis buffer (50 mM Tris–HCl, pH 7.5, 100 mM NaCl, 1 mM EDTA and 1% NP-40) by vortexing 4×30 s with glass beads, using a FastPrep machine (Savant Instruments). The lysis buffer contained a protease inhibitor cocktail (Complete™, Roche) and protein phosphatase inhibitors (10 mM NaF, 10 mM p-nitrophenylphosphate, 10 mM sodium pyrophosphate and 10 mM β-glycerolphosphate). Crude extracts were cleared with a 5-min, 1500 g, spin and the supernatant was used for Western blot analysis as previously described [1], using a mouse monoclonal anti-HA antibody (16B12, BAbCo), a rabbit polyclonal anti-Cdk antibody (for cyclin-dependent kinase; PSTAIRE, Santa Cruz), and a mouse monoclonal anti-3-phosphoglycerate kinase antibody (22C5, Molecular Probes).

2.3. Indirect immunofluorescence

Logarithmically growing cells were fixed for 2 h in growth medium supplemented with formaldehyde (3.7%) and potassium phosphate buffer (100 mM, pH 6.5). The cells were washed and resuspended in sorbitol buffer (1.2 M sorbitol, 100 mM potassium phosphate, pH 6.5). The cell walls were digested for 60–120 min at 37 °C in sorbitol buffer supplemented with 2-mercaptoethanol (20 mM) and Zymolyase 20T (0.1 mg/ml; Seigagaku Corp). Spheroplasts were attached to poly-L-lysine-coated glass slides and permeabilized in PBT (53 mM Na_2HPO_4, 13 mM NaH_2PO_4, 75 mM NaCl, 0.1% Triton X-100). HA-tagged Tat2p was detected with a mouse monoclonal anti-HA antibody (clone 16B12; BAbCO) at a final dilution of 1:500. The samples were treated with primary antibody for 2 h and subsequently with Cy3-conjugated secondary antibody (Molecular Probes, Inc.) at a final dilution of 1:500 for 90 min and 4′,6-diamidino-2-phenylindole (DAPI) for 15 min as described [1]. Washed cells were viewed using an Olympus IX71-23FL/S microscope (100× objective) and a cooled charge-couple device camera (ORCA-ER-1, Hamamatsu Photonics) connected to a Scanalytics Image Processor LuminaVision (Mitani Corp., Tokyo, USA). For double staining of HA-Tat2p and Pep12p, a rabbit polyclonal anti-HA antibody (Y11; Santa Cruz) at a final dilution of 1:500 and a mouse monoclonal anti-Pep12 antibody (Molecular Probes, Inc.) at a final dilution of 1:50 were used. After washing with PBS, cells were treated with Cy3-conjugated anti-rabbit and Alexia 488-conjugated anti-mouse antibodies (Molecular Probes, Inc.) at final dilutions of 1:500. For double staining of HA-Tat2p and alkaline phosphatase (ALP), a rabbit polyclonal anti-HA antibody (Y11; Santa Cruz) at a final dilution of 1:500 and a mouse monoclonal anti-ALP antibody (Molecular Probes, Inc.) at a final dilution of 1:500 were used. After washing with PBS, cells were treated with Cy3-conjugated anti-mouse and Alexia 488-conjugated anti-rabbit antibodies (Molecular Probes, Inc.) at final dilutions of 1:500.

2.4. Tryptophan import activity

Tryptophan import activity of cells was measured as described [19]. Briefly, cells (a 5-ml culture in SD grown to mid-log phase) were collected by centrifugation and washed with 5 ml of SD minus amino acids and finally resuspended in 500 μl of SD minus amino acids. The assay was initiated by the addition of ^{14}C-radiolabeled tryptophan to a final concentration of 4 μM. One hundred-microliter samples were taken at five 1-min intervals and were chilled by the addition of 900 μl of ice-cold SD minus amino acids. The cells were collected by filtration through a nitrocellulose filter (pore size 0.45 μm; Millipore) and washed with 30 ml of chilled water. The filter was dried, and the amount of intracellular labeled tryptophan was estimated by liquid scintillation counting. Experiments were repeated with essentially identical results. Only one set of data is shown here.

2.5. Drug treatments

Stock solutions (at 1000 times the final concentration used) of sterol synthesis inhibitors, zaragozic acid A (ZA; a kind gift from Merck), terbinafine (a kind gift from Novartis), and ketoconazole (ICN) were prepared in water, ethanol, and dimethyl sulfoxide, respectively [20]. Cells were treated with these drugs at the following concentrations: ZA, 10 μg/ml; terbinafine, 50 μg/ml; or ketoconazole, 10 μg/ml [20]. Tests of drug susceptibilities of yeast cells were conducted using cells logarithmically grown in SD medium. Cells were suspended in YPD medium to a concentration of 6×10^6 cells per ml (optical density at 600 nm of 0.2). Cells were plated by transferring 1 μl of the original suspension (10^0) plus 10^{-1} and 10^{-2} dilutions onto YPD plates containing the

drug to be tested. The plates were incubated 2 days at 30 °C and observed for growth. Stock solutions (at 250 times the final concentration used) of the TOR inhibitor rapamycin (Wako, Tokyo) were prepared in 90% ethanol and 10% Tween 20 [1]. Cells were treated with rapamycin at 200 ng/ml.

3. Results and discussion

3.1. ZA compromises Tat2p maintenance and tryptophan uptake

Several kinds of stress induce vacuolar degradation of Tat2p, whereas inhibition of ergosterol biogenesis by the deletion of *ERG6* only impedes plasma membrane trafficking of Tat2p without promoting its vacuolar degradation under high tryptophan conditions (see Introduction). In another line of our study, we also found that *erg6* deletion did not cause Tat2p degradation under normal tryptophan conditions (Fig. 2C). Furthermore, the *ERG* genes encoding enzymes involved in later steps of ergosterol biosynthesis (*ERG6, ERG2*, *ERG3*, *ERG5*, and *ERG4*) (see Fig. 1) are not essential for cell viability, whereas those involved in earlier steps (*ERG9, ERG1*, *ERG7*, and *ERG11*) are required for viability. This suggests that defects in earlier steps of ergosterol biosynthesis may cause different effects on membrane trafficking of proteins than the defect in *ERG6*. We were curious whether this different phenomenon regarding Tat2p is caused by inhibition of earlier steps of ergosterol biosynthesis. In this study, we used tryptophan auxotrophic (*trp1*), not autotrophic (*TRP1)*, cells, and a standard concentration (20 μg/ml) of tryptophan in culture media, in order to be able to compare the results to those of previous studies [1–5,18,21].

Various inhibitors of enzymes involved in the earlier steps are available, including ZA (an inhibitor of SQS encoded by *ERG9*), terbinafine (an inhibitor of squalene epoxidase encoded

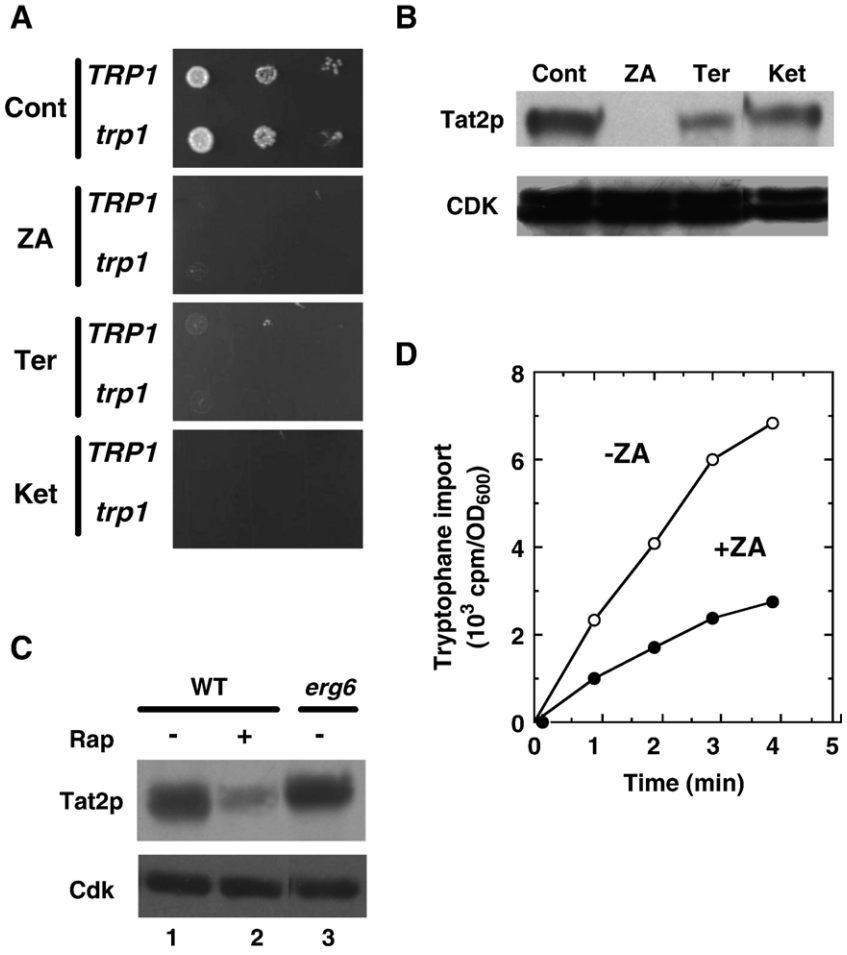

Fig. 2. Reduction of Tat2p protein and tryptophan uptake by inhibitors of sterol biosynthesis. (A) Cell growth inhibition by ergosterol synthesis inhibitors. The wild-type strain (SCU7) cells and cells transformed with plasmid pRS414 (*TRP1 CEN*). Serially diluted cells of each strain were spotted from left to right on YPD plates containing each drug: zaragozic acid (ZA; 10 μg/ml), terbinafine (50 μg/ml), or ketoconazole (10 μg/ml). Plates were cultured at 30 °C for 2 days. (B) Decrease of Tat2p protein by ergosterol synthesis inhibitors. The wild-type strain (KMY1005) harboring plasmid pHA2-TAT2 (pSCU301) was treated with ZA (10 μg/ml), terbinafine (50 μg/ml), or ketoconazole (10 μg/ml) for 3 h, and the protein levels of Tat2p (HA2-Tat2), and cyclin-dependent kinase (CDK; loading control) were examined by Western blotting using anti-HA and anti-CDK antibodies. (C) Tat2p protein is not decreased by *erg6* disruption. The protein levels of Tat2p (HA-Tat2) and CDK in the wild-type (RH2886, lanes 1 and 2) and *erg6* (SCU816, lane 3) strains harboring plasmid pHA2-TAT2 (pSCU301) were determined by Western blotting. For the control, we used cells treated with rapamycin (200 ng/ml) for 1 h (lane 2). (D) Tryptophan uptake declined in the ZA-treated cells. ZA treatment was done as described in panel B. Tryptophan uptake activity was determined as described in Materials and methods. Independent experiments were repeated with essentially identical results. Only one set of data is shown.

by *ERG1*) and ketoconazole (an inhibitor of lanosterol C-14 demethylase encoded by *ERG11*) (see Fig. 1). We treated cells with each drug at the concentration normally used (namely, at which the agent fully inhibits the activity of the corresponding enzyme) [20,22–24]. ZA, terbinafine and ketoconazole completely inhibited cell growth in our strain background. This was the case regardless of whether the cells were in a *TRP1* or *trp1* background (Fig. 2A), consistent with the non-viability of cells deleted for *ERG9*, *ERG1* and *ERG11*. This is in sharp contrast to the fact that the *erg6* cells are viable in a *TRP1*, but not *trp1*, background [2].

In order to assess whether these inhibitors promoted vacuolar degradation of Tat2p, as do nutrient starvation, high tryptophan and high pressure, first we examined the effects of these inhibitors of ergosterol synthesis on Tat2p protein levels. In contrast to *ERG6* disruption (Fig. 2C), which does not cause a decrease in cellular Tat2p protein under tryptophan-sufficient conditions [2], ZA drastically reduced the level of cellular Tat2p protein even if sufficient tryptophan was provided (Fig. 2B). In addition, terbinafine decreased the level to a lesser extent. In contrast, no obvious effect was found in the presence of ketoconazole. Rapamycin immediately promotes the pathway of Tat2p degradation [1]. In contrast, we found that Tat2p was almost lost 3 h after ZA treatment in a preliminary study. This is probably because ergosterol constituents in the cells gradually changed. Cells treated with ZA for 3 h did not lose viability, which was checked by colony formation (data not shown). In order to assess the effect of ZA on Tat2p clearly, we adopted 3 h of ZA treatment.

Thus, the activities of enzymes of early steps of ergosterol biosynthesis, namely, SQS and squalene eposidase, are critical for Tat2p maintenance, unlike sterol C-24 methyltransferase encoded by *ERG6*. Indeed, tryptophan import activity was decreased by the most potent inhibitor, ZA (Fig. 2D). Some residual import activity was detected in the ZA-treated cells in this assay (see below).

3.2. ZA induces vacuolar sorting and degradation of Tat2p

We then focused on further characterizing ZA. Under normal conditions, the plasma-membrane localization of Tat2p was not evident and Tat2p showed a punctate intracellular localization (Fig. 3A). The punctate signals were co-localized with Pep12, the syntaxin that marks late endosomes (Fig. 3A), as described previously [1,2]. This demonstrates that Tat2p is predominantly distributed to late endosomes under normal tryptophan conditions.

We suspected that Tat2p is targeted to and degraded in the vacuoles in ZA-treated cells. Tat2p signals were very weak in most ZA-treated cells (data not shown), consistent with a lowered level of Tat2p protein (see Fig. 2A). However, Tat2p was found to be co-localized with the vacuolar membrane protein alkaline phosphatase (ALP) in some ZA-treated cells (Fig. 3B). This suggests that ZA promotes vacuolar targeting of Tat2p.

To verify this, we examined the effects of deletion of the *PEP4* gene on the decrease in the protein level of Tat2p caused by ZA. *PEP4* encodes the vacuolar protease responsible for the degradation of Tat2p in the vacuole [1,2]. If ZA promotes the vacuolar degradation of Tat2p, the decrease in Tat2p ought to be suppressed by deletion of *PEP4*. This was indeed the case, as *pep4*Δ prevented the ZA-induced reduction of Tat2p (Fig. 3C). Consistent with this, clear vacuolar accumulation of Tat2p was observed in the *pep4* mutants (Fig. 3D). Thus, ZA elicits missorting and vacuolar degradation of Tat2p.

3.3. Rsp5p-mediated ubiquitination of Tat2p is required for the ZA-induced vacuolar missorting of Tat2p

Tat2p vacuolar targeting stimulated by nutrient starvation, high tryptophan, and high pressure is mediated by ubiquitination of Tat2p. This is mediated by the ubiquitin ligase Rsp5p and alleviated by the ubiquitin-specific proteases Doa4p, Ubp6p and Ubp14p [1–4]. The protein kinase TOR (target of rapamycin), which is a central controller of cell growth in response to nutrient availability, controls the vacuolar sorting of Tat2p: rapamycin, a specific inhibitor of TOR, stimulates the vacuolar targeting and degradation of Tat2p [1] (see Fig. 1C). Vacuolar sorting is thought to be primed by Tat2p ubiquitination [1,2], which is prevented by the use of Tat2 (5KR)p, a stabilised version of Tat2p in which five putative ubiquitination target lysine sites in the NH_2-terminus of Tat2p are substituted by arginine. Tat2(5KR)p is predominantly localized to the plasma membrane, and its localization and protein level are resistant to rapamycin. Rapamycin-induced Tat2p degradation is completely suppressed by these mutations. However, substitution of three of these five lysine residues by arginine was sufficient for prevention of the ubiquitination of Tat2p in ERG^+ strains, but not the *erg6* mutant [1,2].

Tat2(5KR)p was clearly observed on the plasma membrane (Fig. 4A), as described previously [1]. It was still localized there even after ZA treatment, in sharp contrast to the wild-type Tat2p. In addition, this mutation suppressed ZA-induced Tat2p degradation, as well as rapamycin-induced one (Fig. 4B). Thus, vacuolar missorting of Tat2p in ZA-treated cells is dependent on its ubiquitination. Furthermore, a conditional mutation allele of *rsp5, rsp5-1*, partially suppressed ZA-induced Tat2p degradation at restrictive temperatures, as well as the rapamycin-induced degradation (Fig. 4B). Based on all these findings, we conclude that ZA-induced vacuolar degradation of Tat2p is dependent on Rsp5p-mediated ubiquitination of Tat2p.

3.4. Vacuolar sorting pathway of Tat2p in ZA-treated cells

Tat2p is sorted from early endosomes either to plasma membranes or to late endosomes, and subsequently targeted to vacuoles [1,2] (see Fig. 8). Rapamycin accelerated sorting of Tat2p from plasma membranes to vacuoles. However, this degradation route is a minor pathway, because massive Tat2p degradation still occurs in the *end4* mutant [1]. It is likely that the massive degradation of Tat2p caused by rapamycin reflects vacuolar degradation of endosomal Tat2p. Similarly, Tat2p

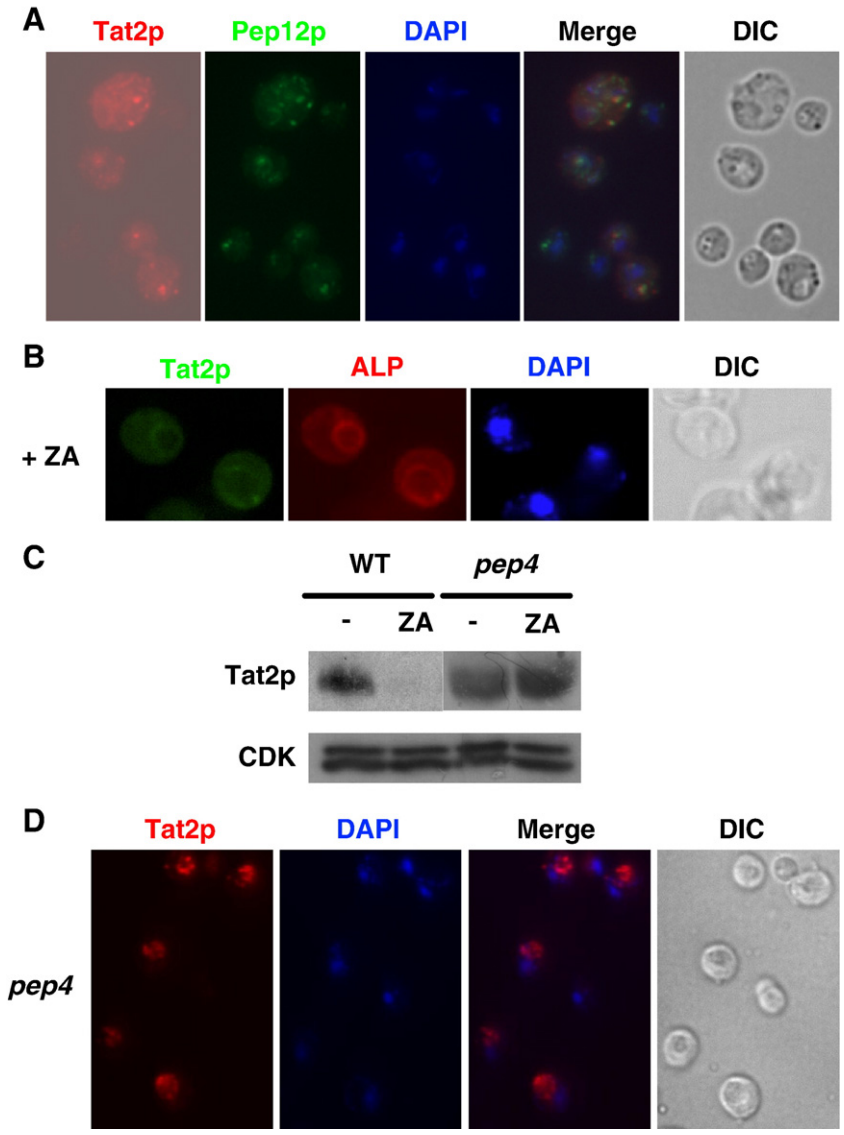

Fig. 3. ZA promotes vacuolar degradation of Tat2p. (A and B) Tat2p localization in cells grown under normal conditions (A) or treated with ZA (10 μg/ml) for 3 h (B). The localization of HA2-Tat2 protein of the-wild type strain (SCU7) harboring plasmid pHA2-TAT2 (pSCU301) was observed by indirect immunofluorescence. (A) Cy3-stained Tat2p (red), Alexia 488-stained Pep12 (green) and DAPI-stained DNA (blue) signals were observed in cells. Nomarski images (DIC) were also recorded. (B) Alexia 488-stained HA2-Tat2 (green), Cy3-stained alkaline phosphatase (ALP; red) and DAPI-stained DNA (blue) signals were observed in cells. (C) The ZA-mediated Tat2p decrease was abolished by disruption of *PEP4*. *pep4* (SCU645) cells harboring plasmid pHA2-TAT2 (pSCU301) were treated with ZA for 3 h and Western blot analysis was done as described in Fig. 2B. (D) Vacuolar localization of Tat2p after ZA treatment in the *pep4* mutant. *pep4* (SCU645) cells harboring plasmid pHA2-TAT2 (pSCU301) were treated with ZA for 3 h and Tat2p (red) and DAPI (blue) signals were observed. (For interpretation of the references to colour in this figure legend, the reader is referred to the web version of this article.)

sorting from early endosomes to vacuoles via late endosomes was stimulated in the *erg6* mutant when the concentration of tryptophan in the culture medium was low [2].

Because ergosterol is required for endocytosis [16,25], it is unlikely that the route from the plasma membrane to the vacuole is stimulated by ergosterol depletion. The ZA-induced decrease in Tat2p was still found in endocytosis-defective *end4* mutants (Fig. 5A). This is probably because Tat2p is predominantly localized in late endosomes, not the plasma membrane (Fig. 3A) [1,2], in a sharp contrast to Tat2 (5KR)p (Fig. 4A). It is possible the massive degradation of Tat2p caused by ZA reflects vacuolar degradation of late endosomal Tat2p. This notion seems to be consistent with the fact that ZA reduces tryptophan uptake activity only by about half, despite the marked decrease in the cellular Tat2p level. The decrease in tryptophan uptake activity after ZA treatment suggests that Tat2p localized on the plasma membrane was decreased. It is probable that Tat2p sorting from early endosomes to late endosomes, but not to plasma membranes, is stimulated by ZA.

To assess the routes of vacuolar degradation of Tat2p, we examined the effect of deletion of *VPS45* on the ZA-mediated Tat2p degradation. Vps45p (VPS for vacuolar protein sorting) is necessary for the delivery of vacuolar proteins from the trans-Golgi network to the pre-vacuolar compartment (PVC), but is not required for the delivery of endocytosed proteins to the

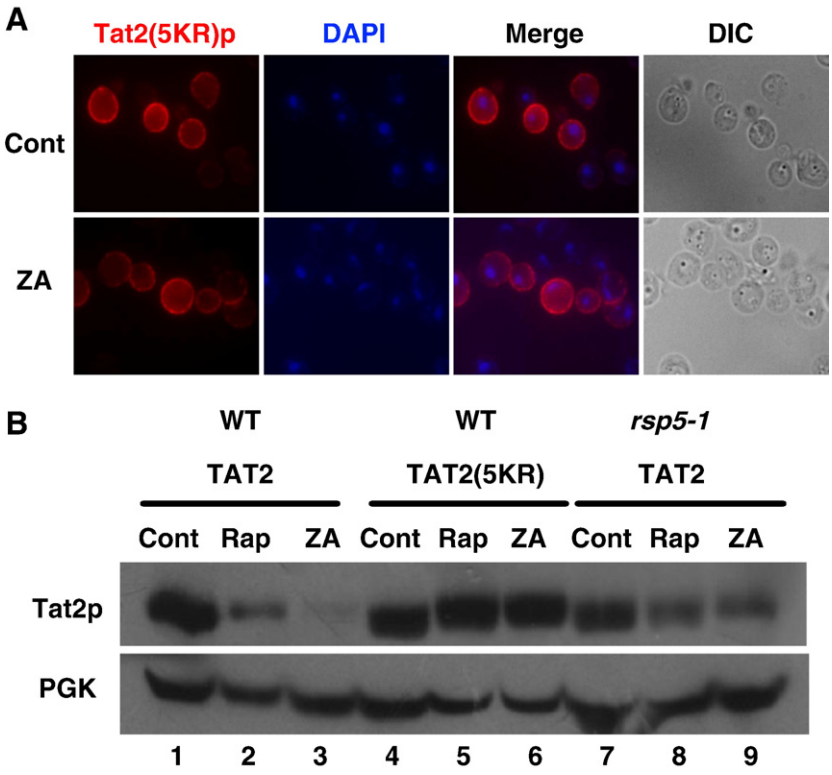

Fig. 4. Ubiquitination-dependent vacuolar missorting of Tat2p in ZA-treated cells. (A) Tat2(5KR) prevents vacuolar targeting of Tat2p in ZA-treated cells. ZA-treated wild-type cells harboring plasmid pHA2-TAT2(5KR) (pSCU425) were treated with ZA for 3 h as described in Fig. 3D. The localization of HA2-Tat2(5KR) was observed by indirect immunofluorescence. Cells not treated with ZA were used as the control (Cont). (B) Tat2(5KR) (lanes 4–6) and *rsp5-1* (lanes 7–9) mutations suppress the ZA-induced Tat2p degradation. ZA-treated cells harboring plasmid pHA2-TAT2 or pHA2-TAT2(5KR) were used for Western blotting. ZA treatment was done as described in Fig. 2B. Cells were treated with rapamycin (1 h) or ZA (3 h). Cont, non-treated control; Rap, rapamycin-treated cells. The *rsp5-1* cells (SCU649) were transferred to 37 °C (restrictive temperature) before drug treatments. PGK (3-phosphoglycerate kinase) was used as the loading control.

vacuole [26]. It has been reported that deletion of *VPS45* suppressed the rapamycin-induced Tat2p degradation [1]. However, the degradation occurred to a similar degree even in the *vps45*-deleted mutant in our cell background (Fig. 5B versus Fig. 2C). It is possible that the different genetic backgrounds of the cells account for these different results. Deletion of *VPS45* also failed to suppress the ZA-induced Tat2p degradation (Fig. 5B). This suggests that the ZA-promoted vacuolar degradation of Tat2p is independent of Vps45p.

The dynamin-related GTPase Vps1p is required for vacuolar sorting from the trans-Golgi to late endosomes [27,28]. Plasma membrane targeting of Tat2p, which is compromised by high tryptophan and *erg6* mutation, is ameliorated by the *vps1* disruption, although there is no reported information about cellular Tat2p protein levels [2]. *PEP12/VPS6* encodes the syntaxin homolog (t-SNARE) Pep12p involved in Golgi-to-vacuole transport [29]. Deletion of *PEP12* partially suppressed the rapamycin-mediated Tat2p degradation [1] and alleviated plasma membrane distribution of Tat2 in the *erg6* mutant [2]. However, in our case, the deletion of *VPS1* and *PEP12* failed to abrogate the rapamycin- and ZA-induced Tat2p degradation (Fig. 5C). Thus, ZA-induced Tat2p degradation is not dependent on Vps1p and Pep12p, at least in our cell background, although the Tat2p distribution in these mutants was not the same as that in the wild-type strain (see below).

Three types of endosome have been characterized: the early/recycling endosome, PVC, and multivesicular body (MVB)/late endosome. MVBs/late endosomes are larger, contain internal vesicles, and are often adjacent to the vacuole. Some vacuolar membrane proteins and internalized surface proteins are sorted into internal vesicles during transport through endosomes in a process known as MVB sorting and are ultimately delivered to the vacuole lumen [30]. Vps27p is required for MVB formation and has been proposed to be an endosomal ubiquitin-sorting receptor [31–34]. Deletion of *VPS*27 cancels Tat2p vacuolar degradation by rapamycin, high tryptophan and high pressure [1–3]. Although deletion of *VPS27* partially suppressed the rapamycin-induced Tat2p degradation, it could not suppress the ZA-induced Tat2p degradation (Fig. 5C). This suggests that another pathway than that involving Vps27p for vacuolar sorting of Tat2p might be activated in the ZA-treated cells. Considering all these facts, it is likely that ZA may induce Golgi-to-vacuole targeting of Tat2p via an aberrant pathway. Thus, we found no obvious suppression of the ZA-induced Tat2p decrease in several mutant cells used here, but it is possible that there are differences of kinetics between the mutants at earlier time points after drug addition.

A relatively large single signal or a few signals of Tat2p in the cell were found in the *vps1*, *vps27* and *vps45* cells (Figs. 6

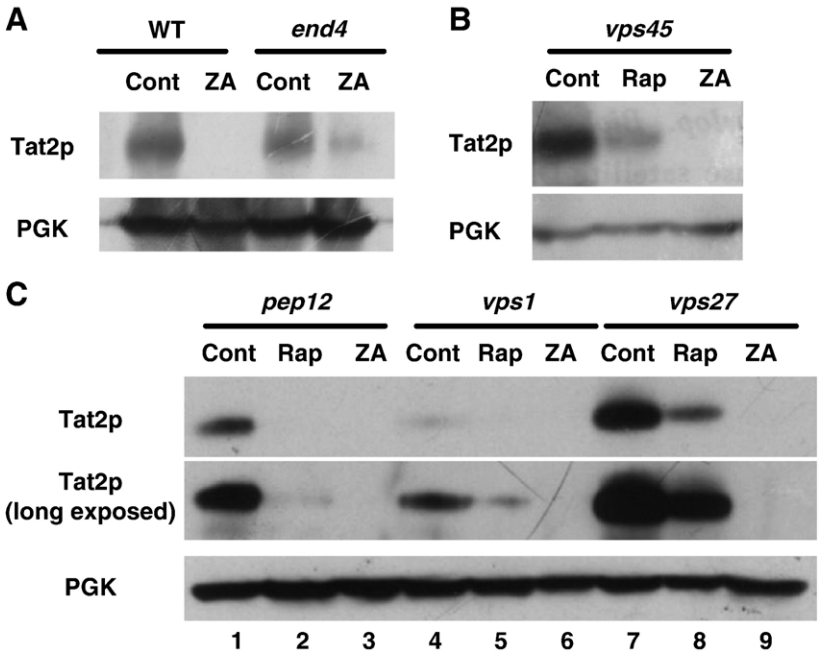

Fig. 5. Effects of deletions of *VPS* genes on ZA-mediated Tat2p degradation. (A–C) Mutant strains *end4* (SCU620), *vps45* (SCU757), *vps1* (SCU718), *vps27* (SCU874) and *pep12* (SCU755) harboring plasmid pHA2-TAT2p (pSCU301) were treated with rapamycin (1 h) and ZA (3 h). Tat2p (HA-Tat2p) was detected by Western blot analysis as described in Fig. 4B.

and 7A). Thus, Vps1, Vps27 and Vps45 are involved in proper localization of Tat2p. These signals were co-localized with Pep12p. It was previously shown that Pep12p is missorted in *vsp1*, *vps27* and *vps45* cells [35–37]. In contrast, punctate signals of Tat2p were observed in the *pep12*, even after ZA treatment (Fig. 7B). It has been reported that deletions of *VSP1*, *VPS27* and *PEP12* promote plasma membrane localization of green fluorescent protein (GFP)-tagged Tat2p (Tat2p-GFP) [2].

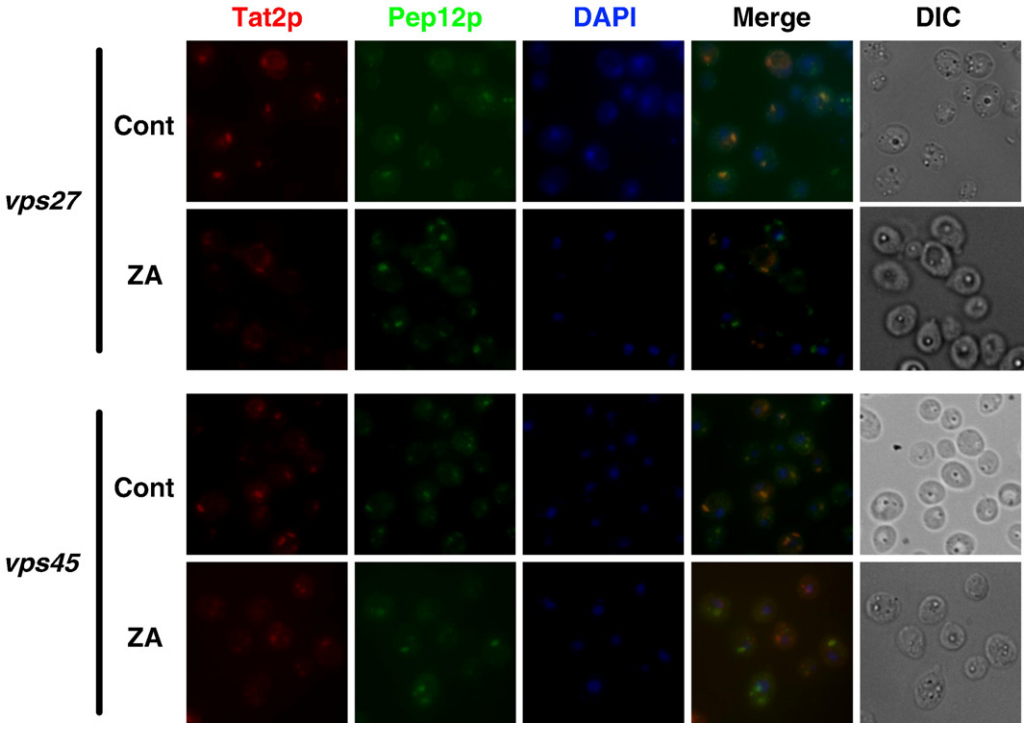

Fig. 6. Tat2p distribution in *vps27* and *vps45*. Mutant strains *vps27* (SCU874) and *vps45* (SCU757) harboring plasmid pHA2-TAT2p (pSCU301) were treated with ZA for 3 h. The localization of Tat2p was observed by indirect immunofluorescence as described in Fig. 3A.

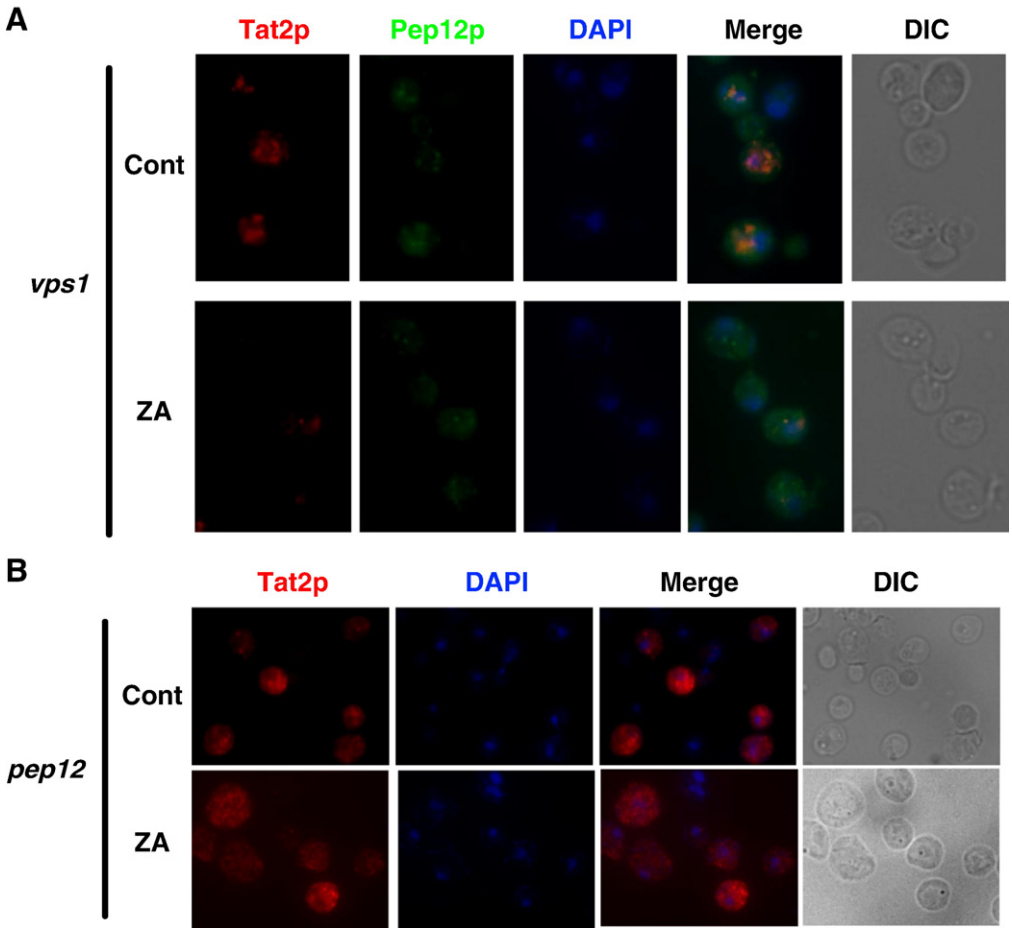

Fig. 7. Tat2p distribution in *vps1* and *pep12*. Mutant strains *vps1* (SCU718) (A) and *pep12* (SCU755) (B) harboring plasmid pHA2-TAT2p (pSCU301) were treated with ZA for 3 h. The localization of Tat2p was observed by indirect immunofluorescence as described in Fig. 3A.

Tat2p-GFP complemented the growth defects of the *tat2*Δ under low tryptophan conditions, like HA-tagged Tat2p [2]. However, this only suggests that Tat2p-GFP can be localized on the plasma membrane regardless of the intracellular distribution of Tat2p. Indeed, the distribution of Tat2p-GFP was not the same as that of Tat2p-HA [2]. It is likely that the difference of tags of Tat2p may have resulted in the difference of the effects of the deletions of *vps1*, *vps27* and *pep12*. It may be useful to analyze endogenous non-tagged Tat2p to exclude effects of tags.

3.5. A model of ZA effect on Tat2p sorting

We showed herein that the SQS inhibitor ZA evoked massive vacuolar degradation of Tat2p. This feature is in contrast to that seen in the *erg6* mutants. Tat2p is predominantly distributed in late endosomes [2] (this study). Therefore, the ZA-induced Tat2p degradation indicates that ZA, but not the *erg6* deletion, promotes late endosomal Tat2p degradation (Fig. 8). Furthermore, the fact that ZA represses tryptophan uptake (Fig. 2D) suggests that ZA inhibits the sorting of Tat2p from the early endosome to the plasma membrane (Fig. 8), like deletion of *ERG6*. This plasma membrane sorting is accelerated by inhibition of Rsp5p-mediated ubiquitination of Tat2p even in the presence of ZA, suggesting that Rsp5p-mediated ubiquitination of Tat2p may inhibit the plasma membrane sorting of Tat2p (Fig. 8).

Cholesterol (ergosterol) and sphingolipids are thought together to form tightly packed lipid microdomains, called “lipid

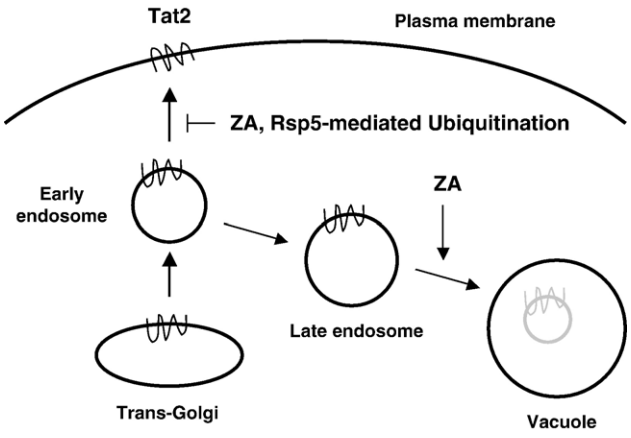

Fig. 8. Model for Tat2p sorting in ZA-treated cells. See the text for details.

rafts". Lipid rafts are critical for intracellular protein sorting [38–42]. Tat2p is also associated with lipid rafts under low, but not high, tryptophan conditions [2,3]. It is likely that zymosterol (see Fig. 1)-containing lipid rafts in the *erg6* mutants stimulate the sorting of Tat2p from early to late endosomes, but not from late endosomes to vacuoles. In contrast, the lack of sterol, unlike zymosterol, in the ZA-treated cells probably promotes both sorting pathways.

3.6. Concluding remarks

The ZA-induced degradation of Tat2p was dependent on the ubiquitination of Tat2p, but may not occur via normal vacuolar sorting pathways. In the case of ZA-mediated ergosterol depletion, Tat2p may be the Achilles' heel of growth, as it is in the case of high pressure [5]. Nutrient uptake is specifically impeded in ergosterol-depleted cells. It is plausible that there is a physiological system that regulates the sorting of nutrient transporters by altering sterol synthesis. In support of this notion, we have found that novel TOR-controlled transcriptional regulators which are needed for full expression of *ERG* genes preferentially control the Golgi-to-plasma membrane sorting of Tat2p (our unpublished data). We suspect that TOR regulates Tat2p sorting via these novel factors and are now investigating this. This control seems to be different from the TOR-regulated Tat2p sorting via protein kinase Npr1p proposed in a previous study [18]. The highly conserved membrane trafficking system implies that similar regulatory systems may exist in other organisms, including humans. Furthermore, this study suggests that high cholesterol may guarantee high nutrient import into cells, and that drugs used to control cholesterol levels could specifically regulate cellular nutrient import in humans.

Acknowledgements

We thank M. Hall (TAT2 plasmids), F. Abe (*rsp5-1* plasmid and anti-Pep12p antibody), S. Helliwell (anti-ALP antibody), Merck (ZA) and Novartis (terbinafine), for materials, H. Riezman, K. Umebayashi and A. Nakano for helpful discussions, and R. Loewith for careful reading of the manuscript.

References

[1] T. Beck, A. Schmidt, M.N. Hall, Starvation induces vacuolar targeting and degradation of the tryptophan permease in yeast, J. Cell Biol. 146 (1999) 1227–1238.
[2] K. Umebayashi, A. Nakano, Ergosterol is required for targeting of tryptophan permease to the yeast plasma membrane, J. Cell Biol. 161 (2003) 1117–1131.
[3] F. Abe, H. Iida, Pressure-induced differential regulation of the two tryptophan permeases Tat1 and Tat2 by ubiquitin ligase Rsp5 and its binding proteins, Mol. Cell. Biol. 23 (2003) 7566–7584.
[4] T. Miura, F. Abe, Multiple ubiquitin-specific protease genes are involved in degradation of yeast tryptophan permease Tat2 at high pressure, FEMS Microbiol. Lett. 239 (2004) 171–179.
[5] F. Abe, K. Horikoshi, Tryptophan permease gene TAT2 confers high-pressure growth in *Saccharomyces cerevisiae*, Mol. Cell. Biol. 20 (2000) 8093–8102.
[6] R.F. Gaber, D.M. Copple, B.K. Kennedy, M. Vidal, M. Bard, The yeast gene *ERG6* is required for normal membrane function but is not essential for biosynthesis of the cell-cycle-sparking sterol, Mol. Cell. Biol. 9 (1989) 3447–3456.
[7] G.W. Robinson, Y.H. Tsay, B.K. Kienzle, C.A. Smith-Monroy, R.W. Bishop, Smith-Monroy, R.W. Bishop, Conservation between human and fungal squalene synthetases: similarities in structure, function, and regulation, Mol. Cell. Biol. 13 (1993) 2706–2717.
[8] J.L. Goldstein, M.S. Brown, Regulation of the mevalonate pathway, Nature 343 (1990) 425–430.
[9] M.S. Brown, J.L. Goldstein, Multivalent feedback regulation of HMG CoA reductase, a control mechanism coordinating isoprenoid synthesis and cell growth, J. Lipid Res. 21 (1980) 505–517.
[10] J.R. Faust, J.L. Goldstein, M.S. Brown, Squalene synthetase activity in human fibroblasts: regulation via the low density lipoprotein receptor, Proc. Natl. Acad. Sci. U. S. A. 76 (1979) 5018–5022.
[11] E. Bruenger, H.C. Rilling, Prenyltransferase and squalene synthetase in livers of neonate rats, Biochim. Biophys. Acta 876 (1986) 500–506.
[12] K. Mori, T. Kawahara, H. Yoshida, H. Yanagi, T. Yura, Signalling from endoplasmic reticulum to nucleus: transcription factor with a basic-leucine zipper motif is required for the unfolded protein-response pathway, Genes Cells 1 (1996) 803–817.
[13] M.S. Longtine, A. McKenzie III, D.J. Demarini, N.G. Shah, A. Wach, A. Brachat, P. Philippsen, J.R. Pringle, Additional modules for versatile and economical PCR-based gene deletion and modification in *Saccharomyces cerevisiae*, Yeast 14 (1998) 953–961.
[14] U. Guldener, S. Heck, T. Fielder, J. Beinhauer, J.H. Hegemann, A new efficient gene disruption cassette for repeated use in budding yeast, Nucleic Acids Res. 24 (1996) 2519–2524.
[15] A.L. Goldstein, J.H. McCusker, Three new dominant drug resistance cassettes for gene disruption in *Saccharomyces cerevisiae*, Yeast 15 (1999) 1541–1553.
[16] A.L. Munn, A. Heese-Peck, B.J. Stevenson, H. Pichler, H. Riezman, Specific sterols required for the internalization step of endocytosis in yeast, Mol. Biol. Cell 10 (1999) 3943–3957.
[17] R.S. Sikorski, P. Hieter, A system of shuttle vectors and yeast host strains designed for efficient manipulation of DNA in *Saccharomyces cerevisiae*, Genetics 122 (1989) 19–27.
[18] A. Schmidt, T. Beck, A. Koller, J. Kunz, M.N. Hall, The TOR nutrient signalling pathway phosphorylates NPR1 and inhibits turnover of the tryptophan permease, EMBO J. 17 (1998) 6924–6931.
[19] K.J. Roberg, N. Rowley, C.A. Kaiser, Physiological regulation of membrane protein sorting late in the secretory pathway of *Saccharomyces cerevisiae*, J. Cell Biol. 137 (1997) 1469–1482.
[20] M.A. Kennedy, M. Bard, Positive and negative regulation of squalene synthase (ERG9), an ergosterol biosynthetic gene, in *Saccharomyces cerevisiae*, Biochim. Biophys. Acta 1517 (2001) 177–189.
[21] A. Schmidt, M.N. Hall, A. Koller, Two FK506 resistance-conferring genes in *Saccharomyces cerevisiae*, TAT1 and TAT2, encode amino acid permeases mediating tyrosine and tryptophan uptake, Mol. Cell. Biol. 14 (1994) 6597–6606.
[22] M.A. Kennedy, R. Barbuch, M. Bard, Transcriptional regulation of the squalene synthase gene (ERG9) in the yeast *Saccharomyces cerevisiae*, Biochim. Biophys. Acta 1445 (1999) 110–122.
[23] D. Zweytick, C. Hrastnik, S.D. Kohlwein, G. Daum, Biochemical characterization and subcellular localization of the sterol C-24(28) reductase, Erg4p, from the yeast *Saccharomyces cerevisiae*, FEBS Lett. 470 (2000) 83–87.
[24] J.H. Crowley, S. Tove, L.W. Parks, A calcium-dependent ergosterol mutant of *Saccharomyces cerevisiae*, Curr. Genet. 34 (1998) 93–99.
[25] A. Heese-Peck, H. Pichler, B. Zanolari, R. Watanabe, G. Daum, H. Riezman, Multiple functions of sterols in yeast endocytosis, Mol. Biol. Cell 13 (2002) 2664–2680.
[26] N.J. Bryant, R.C. Piper, S.R. Gerrard, T.H. Stevens, Traffic into the prevacuolar/endosomal compartment of *Saccharomyces cerevisiae*: a VPS45-dependent intracellular route and a VPS45-independent, endocytic route, Eur. J. Cell Biol. 76 (1998) 43–52.
[27] S.F. Nothwehr, E. Conibear, T.H. Stevens, Golgi and vacuolar membrane proteins reach the vacuole in *vps1* mutant yeast cells via the plasma membrane, J. Cell Biol. 129 (1995) 35–46.

[28] X. Yu, M. Cai, The yeast dynamin-related GTPase Vps1p functions in the organization of the actin cytoskeleton via interaction with Sla1p, J. Cell Sci. 20 (2004) 3839–3853.
[29] J.E. Gerst, SNAREs and SNARE regulators in membrane fusion and exocytosis, Cell Mol. Life Sci. 55 (1999) 707–734.
[30] R.C. Piper, J.P. Luzio, Late endosomes: sorting and partitioning in multivesicular bodies, Traffic 2 (2001) 612–621.
[31] C.K. Raymond, I. Howald-Stevenson, C.A. Vater, T.H. Stevens, Morphological classification of the yeast vacuolar protein sorting mutants: evidence for a prevacuolar compartment in class E vps mutants, Mol. Biol. Cell 3 (1992) 1389–1402.
[32] N.J. Bryant, T.H. Stevens, Vacuole biogenesis in *Saccharomyces cerevisiae*: protein transport pathways to the yeast vacuole, Microbiol. Mol. Biol. Rev. 62 (1998) 230–247.
[33] P.S. Bilodeau, J.L. Urbanowski, S.C. Winistorfer, R.C. Piper, The Vps27p Hse1p complex binds ubiquitin and mediates endosomal protein sorting, Nat. Cell Biol. 4 (2002) 534–539.
[34] S.C. Shih, D.J. Katzmann, J.D. Schnell, M. Sutanto, S.D. Emr, L. Hicke, Epsins and Vps27p/Hrs contain ubiquitin-binding domains that function in receptor endocytosis, Nat. Cell Biol. 4 (2002) 389–393.
[35] M.W. Black, H.R. Pelham, A selective transport route from Golgi to late endosomes that requires the yeast GGA proteins, J. Cell Biol. 151 (2000) 587–600.
[36] S.R. Gerrard, A.B. Mecklem, T.H. Stevens, The yeast endosomal t-SNARE, Pep12p, functions in the absence of its transmembrane domain, Traffic 1 (2000) 45–55.
[37] M.E. Abazeed, J.M. Blanchette, R.S. Fuller, Cell-free transport from the trans-Golgi network to late endosome requires factors involved in formation and consumption of clathrin-coated vesicles, J. Biol. Chem. 280 (2005) 4442–4450.
[38] E. Ikonen, Roles of lipid rafts in membrane transport, Curr. Opin. Cell Biol. 13 (2001) 470–477.
[39] K. Simons, E. Ikonen, How cells handle cholesterol, Science 290 (2000) 1721–1726.
[40] K. Simons, E. Ikonen, Functional rafts in cell membranes, Nature 387 (1997) 569–572.
[41] D.A. Brown, E. London, Structure and function of sphingolipid- and cholesterol-rich membrane rafts, J. Biol. Chem. 275 (2000) 17221–17224.
[42] D.A. Brown, E. London, Functions of lipid rafts in biological membranes, Annu. Rev. Cell Dev. Biol. 14 (1998) 111–136.